

## **THE ENGINEERING AND CONSTRUCTION OF A PRE-BUNCHED FREE ELECTRON MASER**

**F. Malek**

Universiti Malaysia Perlis (UniMAP)  
School of Computer and Communication Engineering  
No. 12 & 14, Jalan Satu, Taman Seberang Jaya Fasa 3  
Kuala Perlis 02000, Perlis, Malaysia

**J. Lucas and Y. Huang**

Department of Electrical Engineering and Electronics  
The University of Liverpool  
Brownlow Hill, Liverpool L69 3GJ, United Kingdom

**Abstract**—We are developing prototype free electron maser (FEM) that is compact, tuneable and efficient for potential industrial use. Therefore we define the characteristics for the construction of a novel X-band rectangular waveguide pre-bunched free electron maser (PFEM). Our device operates at 10 GHz and employs two rectangular waveguide cavities (one for velocity modulation and the other for energy extraction). The electron beam used in this experiment is produced by thermionic electron gun which can operate at 3 kV and up to 5 mA. The resonant cavity consists of a thin gap section of height 1.5 mm which reduces the beam energy required for beam wave interaction. The prototype design, engineering and construction process are reported in this paper.

### **1. INTRODUCTION**

The free electron maser (FEM) is a source of microwave power which makes use of the interaction between the electron beam and electromagnetic radiation [1]. The conventional free electron laser (FEL) consists of three main components: an electron beam in vacuum, a magnetic wiggler or undulator, which stimulates the electron to emit radiation and an optical cavity formed by two mirrors, which

---

Corresponding author: F. Malek (mfareq@unimap.edu.my).

contains and builds up the radiation. In our project, the radiation is at microwave frequencies, therefore, the mirrors will be replaced by a resonant waveguide cavity, and the term free electron maser (FEM) is used.

When an electron passes through the wiggler magnet it oscillates from side to side. The electron radiates an electromagnetic wave but at a higher frequency than the wiggler frequency. The electron radiates almost uniformly from one end of the wiggler to the other and the resulting wave packet contains only a finite number of oscillations [2]. The wave packet has an almost square envelope. Hence its Fourier transform results to a  $\text{sinc}^2$  intensity spectrum. This is called the spontaneous emission and is not coherent. This is because the electrons position in the beam are random, which results in random phases between the EM wave which they emit. The total radiated power is proportional to the number of electrons in the beam, i.e., the beam current, and is weak [3–5].

The purpose of this research is to produce a cost effective FEM, for which the FEM offers the prospect of a microwave source with a broad tuning range, high power and reasonable efficiency which is higher than other conventional FEL or microwave devices. We are developing a novel pre-bunched free electron maser (PFEM) operating at a relatively low voltage of 3 kV at a frequency of 10 GHz. The result is a compact, powerful, efficient and cost effective device suitable for potential industrial applications, such as plasma welding torch, pollution control, microwave processing of materials, detection of shallow buried non-metallic landmine and communication systems [6–8]. The system, shown in Figure 1, consists of a rectangular cavity (for velocity modulation of the electron beams) and a rectangular cavity (for energy extraction). The experimental result demonstrated coherent emission and gain with a beam current of up to 5 mA [9].

The PFEM operates at a low current and accelerating voltage, thus maintaining a compact design. The acceleration potential is applied between the electron gun filament and input cavity. The same X-band microwave source is fed into both the cavities, to ensure the EM wave in both cavities are in phase. The phases of the EM waves can be modified (tuned) by employing a phase shifter. Electron beam passing through the EM wave in the input cavity will be velocity modulated. This velocity modulated electron beam interacts with the EM wave in the output cavity. A strong coherent radiation will be emitted if the velocity modulated electron beam is in phase with the EM wave in the output cavity. As a result, enlarged microwave power can be obtained [10–12].

## 2. PFEM DESIGN CONCEPT

The PFEM structure consists of an input cavity and an output cavity, as can be seen in Figure 1. Each cavity is made of three sections: the standard X-band section, taper section and the thin gap section. The PFEM operates in the X-band spectrum, with a 10 GHz operating frequency. The standard X-band section acts as an interface of PFEM with other waveguide components operating in X-band spectrum. These waveguide components are the E-H tuner, phase shifter, ferrite isolator, Moreno cross-coupler and the X-band source itself.

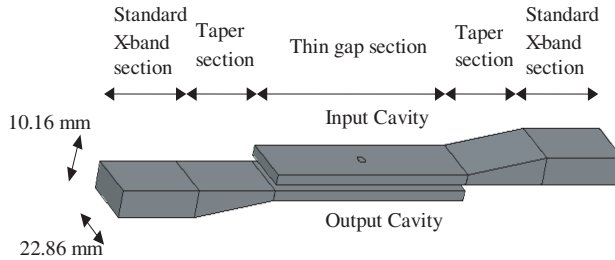


**Figure 1.** Diagram of PFEM showing the input cavity and output cavity.

The end of the thin gap section is terminated by a copper wall. This is to produce a standing EM wave condition in the cavity. The  $TE_{10}$  mode EM wave is generated from an X-band source and travels into the cavity via the opening on standard X-band section [13–16]. A taper section is designed to connect the standard X-band section and the thin gap section. The waveguide of the taper section is designed such that the dimension varies smoothly. This allows a smooth transition of EM wave fed from the input of the standard X-band section to the thin gap section [17]. For each cavity, apertures of 1.5 mm diameter are drilled at the centre of thin gap sections (on both sides of the thin gap sections). An electron gun source (the tip of the filament) is placed at a short distance from the input cavity. Electron beams are emitted from this electron gun source when heated. Strong interaction between the electron beam and EM wave can occur because the path of the electron beam is in parallel  $TE_{10}$  mode field of the EM wave. Moreover, the cavity apertures are located at the centre of the narrow length of the cavity. This ensures that the strongest  $E$ -field of the  $TE_{10}$  mode EM wave will interact with the electron beam [18].

The height of the thin gap section is designed at 1.5 mm, so as to increase the intensity of the  $E$ -field strength, and allows short electron transit time. This height of the thin gap section is chosen so that the

transit time of electron in the thin gap section of the PFEM waveguide must be less than the time for half of a wavelength of the standing wave sinusoidal waveform. The electrons are velocity modulated by the intense EM wave strength in the thin gap section. In other words, the electron beams are pre-bunched by the EM wave in the input cavity. At the same instance, the same EM wave fed into the input cavity from the X-band source is coupled out via a Moreno cross-coupler and coaxial cable and fed into the output cavity.

A phase shifter is placed at the output cavity, where the phase of the EM waves between the two cavities can be varied from 0 to 360 degrees. The phase in between the two cavities are varied so that, bunched electrons will arrive at the output cavity having the same phase as the EM wave, to allow synchronism with the EM wave which results in amplification of the EM wave in the output cavity.

### 3. PFEM EXPERIMENTAL IMPLEMENTATION

#### 3.1. PFEM System Arrangement

The PFEM system set-up, shown in Figure 2, consists of four main components: the electron gun, the input cavity (electron velocity modulator), the output cavity (energy extractor) and the turbo-molecular vacuum pump system. This section describes briefly these components. A simple electron gun arrangement has been used, which incorporates a cathode and an anode. The cathode is designed initially from tungsten filament (operated up to 50  $\mu$ A). At the next stage, Thoria coated Iridium filament has been used as the electron gun source. The input cavity also performs as an anode. The electron gun is operated at voltages up to 3 kV. The supply polarity is negative [18]. The filament is powered using a VARIAC (variable auto transformer) and a step down filament transformer. The output lines of the transformer are connected to the filament.

The electron gun is placed at a short distance before the input cavity. The output cavity is placed directly below the input cavity, as shown in Figures 1 and 2. The two cavities are separated by silicon 'O' ring for insulation purpose. The insulation is needed to allow the current flowing through the apertures to be measured. This input cavity is designed using a standard X-band waveguide, WR90/WG16, with internal broad dimension of 22.86 mm, and narrow dimension of 10.16 mm. As can be seen in Figure 1, each cavity consists of three main sections: the standard X-band section, the tapered section and the thin gap section.

Based on the operating frequency of 10 GHz, the length of the standard X-band section is designed to be one waveguide

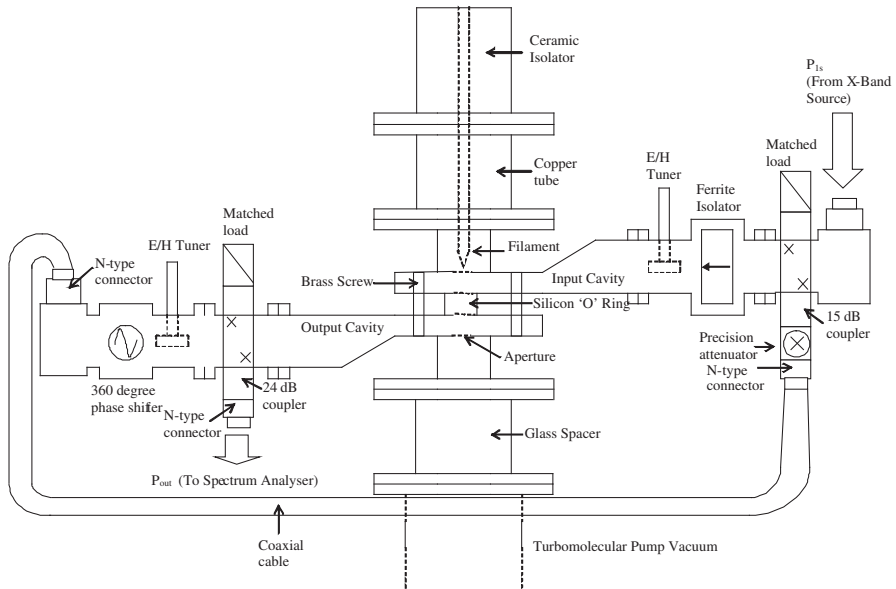


**Figure 2.** Diagram of pre-bunched free electron maser (PFEM) system. The electron gun and high voltage circuits are omitted for simplicity purpose.

wavelength ( $\lambda_g$ ). A thin gap section of height 1.5 mm and length  $2.5 \times \lambda_g$  waveguide wavelength ( $2.5 \times \lambda_g$ ) is connected to the tapered section. Apertures of 1.5 mm diameter are drilled in the centre of the thin gap section to allow electrons to flow through, and hence pre-bunched by the EM wave in the input cavity.

Therefore, a tapered section of one waveguide wavelength ( $\lambda_g$ ) is placed in between the standard X-band section and the thin gap section. The taper should be designed to keep radiation reflection loss at a minimum, since the power may be lost to reflection and radiation [13–16]. Simulation using Vector Fields CONCERTO shows that the return loss of EM wave is minimized when the taper length is designed to be equal to  $1 \times$  waveguide wavelength.

The microwave power (up to 10 dBm) from the Marconi signal generator is fed into input cavity. To ensure the same phase, the same microwave power is fed into the output cavity using the 15 dB coupler, via a coaxial cable. The two cavities are further fully tuned to get the best resonance by using E-H tuners. The operating frequency is fixed at 10 GHz. A 360 degree phase shifter, placed at the output cavity, can be adjusted to ensure the correct phase between the bunched electron

beams and the microwave  $E$ -field in the output cavity. The bunched (velocity modulated) electron beams will travel from the apertures of the input cavity into the apertures of the output cavity. These bunched beams will strongly interact with the  $TE_{10}$  mode  $E$ -field wave in the output cavity. The resultant microwave signal in the output cavity is extracted to the spectrum analyzer for analysis using a 24 dB Moreno cross coupler. To measure the current flowing across the apertures of the output cavities, a glass spacer is placed in between the output cavity and the turbo molecular vacuum pump. This glass spacer also provides additional security, as it separates the vacuum pump from the PFEM cavities and the high voltages.

### 3.2. Main Body of the PFEM

The resonant cavities of the PFEM are constructed from the WR90 rectangular waveguide (X-band frequency region). Rectangular waveguide was chosen in this project to overcome overmoding problems [19–21]. The constructions of various PFEM components are described in this paper.

The main body of the PFEM device is constructed from a long X-band rectangular waveguide. The diagram of the long X-band rectangular waveguide is shown in Figure 3, where the dotted line shows the section of this waveguide to be cut using the milling cutter. The horizontal length of the thin gap section is designed to be  $2.5 \cdot \lambda_g$ , while the horizontal lengths of the taper section and the standard X-band section are  $\lambda_g$  respectively. After cutting this waveguide, if one is to view the end result from the top (aerial view), the thin gap section and the taper section are now ‘topless’. In order to cover these two ‘topless’ sections, copper plates will be placed on top of the respective sections. These copper plates were aluminum soldered along the edges. It is shown that leaks occurred along the edges when this aluminum soldering was used.

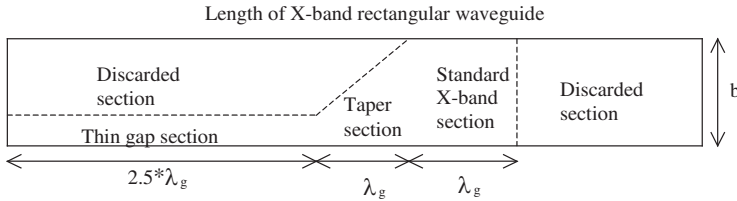


**Figure 3.** Diagram (side view) of a long X-band rectangular waveguide where the PFEM waveguide cavity will be constructed from it.

As a solution, soft soldering (60% tin / 40% lead) was used and no leaks occurred. The soft soldering procedure was performed at about 2000 Celsius. Due to cost reasons, the soldering method was used in constructing the cavity instead of the welding method. After covering the two sections (taper section and thin gap section) with thin copper plates, there still left an open air at the end of the thin gap section. In order to resonate, the cavity requires “mirror” at each end. These mirrors are needed to reflect the microwave radiation. In microwave frequencies, this can be provided by the short circuit wall at one end and an isolator at the other end which allows microwave in one direction and not the opposite direction.

Therefore, another thin copper plate was cut from an existing X-band waveguide, and this copper plate (1.5 mm width and 22.86 mm length) was soft soldered onto the end (open air) of the thin gap section. Apertures of 4 mm diameter are required to be placed at the centre of the thin gap section at both cavities. These 4 mm diameter apertures were drilled at the centre of the thin gap section of both cavities.

### 3.3. Filament Housing

The filament would need to be placed just before the aperture of the input cavity. The filament needed to be housed by a suitable material component to preserve the vacuum condition for the filament to operate in optimum condition. A copper tube is used to house the filament. The outer diameter of this copper tube was measured at 22 mm. The diameter of the copper tube was larger than the aperture diameter (4 mm) on the thin gap section, but smaller than the wide dimension of the X-band rectangular waveguide (22.86 mm). This copper tube was cut from the available long copper tube. It was cut at the centre. One copper tube was for the input cavity (for filament housing), and another copper tube was for the output cavity (for connection to glass spacer).

The cut length of the copper tube was measured appropriately so that the length of the filament and its copper wires can be placed comfortably in it. One end of the copper tube is silver soldered to a 70 mm diameter standard vacuum flange (DN40CF). Silver solder was used for soldering copper to steel material such as the vacuum flange. The temperature used for silver soldering was at 6000 Celsius, which was much higher than that of soft soldering. The other end of the copper tube was soft soldered on top of the thin gap section surface, encircling the aperture of the input cavity. The total distance from the vacuum flange of the copper tube to the surface of the thin gap section is measured at 48 mm.

### 3.4. The Silica Windows

In the input cavity, microwave EM wave enters through an aperture on one side of the cavity. The waveguide feeding the cavity from the microwave source is not evacuated. Hence, a silica window is bonded to the cavity to seal the input power aperture. The silica does not affect the microwave transmission significantly due to its low-loss dielectric characteristic. The output cavity also has a silica window seals on the output power aperture side. One end of the input cavity and output cavity was soft soldered to standard UBR100 waveguide flanges respectively, which can be seen in Figure 4. A 2 mm gap was left before the end of the waveguide cavity. This space is designated for the silica window that will terminate the waveguide cavity. These windows allow transition from the vacuum system of the resonant cavity to standard waveguide components in atmosphere.

The UV fused silica window is of 40 mm diameter and 2 mm thickness. Two rectangular shapes, with 24.5 mm length and 12 mm width each, as shown in Figure 5 were cut at the glass workshop. Epoxy Araldyte adhesive was placed along the ridge of the waveguide cavity. The silica window was then placed on top of the waveguide ridge. The silica window was left for overnight for drying. The same procedure was applied to the other waveguide cavity. The windows are now secured to the respective waveguide flanges using the epoxy Araldyte adhesives. It should be noted that the use of soft-soldering or epoxy adhesives are not recommended for high vacuum components as both soldering resin residues and epoxy out-gas quite badly. However, this is compensated by the high capacity of the vacuum pumping system.

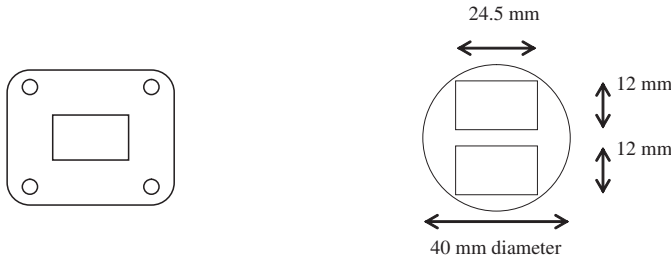


**Figure 4.** UBR100 standard waveguide flange.

**Figure 5.** Two rectangular shapes cut from a circular UV fused silica window.



### 3.5. The Tightening of the Two Cavities

The now completed waveguide cavities (input cavity and output cavity) can be placed on top of each other. For monitoring the current flow across the apertures, a PTFE layer is placed in between the two cavities. Silicon 'O' ring was placed in between the two cavities for vacuum sealing purpose. Two brackets and four brass screws and nuts were used to clamp the two cavities together. The length of each bracket is 5 mm and its width is 1.5 mm. The length of each brass screw is 4.1 mm. Two holes were drilled at each bracket near to each end of the bracket. The brass screw could then be slotted into the hole of one bracket, and to the hole of another bracket located below the first bracket. The holes on the two brackets were aligned with each other, so that the brass screws could be slotted perfectly into the two brackets. Nut was used to tighten the two brackets. The same procedure is applied to the other two brackets. The completed construction of the input and output cavities is shown in Figure 6.

### 3.6. The Filament Circuit Housing

Section 3.3 describes the cavity construction for housing the filament which is placed just before the aperture of the input cavity. A method is also needed to house the copper wires, the copper base and stanchions from the flange base. As a summary, these components can be called the filament circuit elements. A 70 mm diameter copper tube is used to house the filament circuit housing. This copper tube was cut to 73 mm length. The copper tube was then silver soldered to two 70 mm diameter vacuum flanges (DN40CF) at both of its ends. Test performed indicated that the vacuum pressured was lowered to a satisfactory level ( $1 \times 10^{-8}$  mbar). Hence no leakages were found in the constructed copper tube with vacuum flanges.

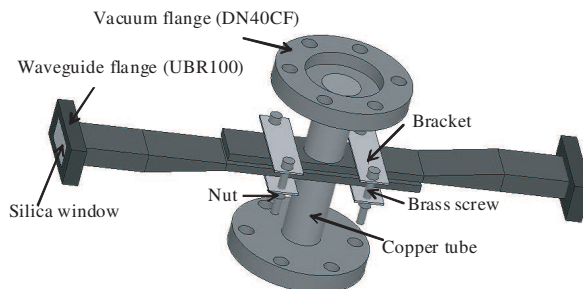


**Figure 6.** Completed PFEM consisting of input and output cavities, clamped by brackets, brass screws and nuts.

### 3.7. The Glass Spacer

The current flow across the apertures of the output cavity needed to be monitored for beam line measurement. If the output cavity is connected directly to the vacuum pump, this aperture current cannot be measured because the current will flow onto the vacuum pump and to the earth. This is because the vacuum pump is placed at the earth potential. The solution is to place a glass tube in between the output cavity and the vacuum pump, so that an ammeter can be placed in between the output cavity and the earth to measure the current flowing across the apertures of the output cavity.

This glass tube was cut to a length of 40 mm from an existing available long glass tube. Epoxy Araldyte adhesive were placed along the ridges of the two vacuum flanges (DN40CF). Each end of the glass tube was placed on top of each of the vacuum flange ridge. The glass tube was left for overnight for drying. In the next morning, the glass tube is now secured to the vacuum flanges using epoxy Araldyte adhesives.

### 3.8. Electron Gun

An electron gun was designed, constructed and tested that can provide up to few mA of beam current at a nominal voltage of 3 kV. In the initial stage, tungsten filament is used as the electron gun source (cathode). As the initial result showed potential, Thoria coated iridium filament (cathode) is used as the electron gun in the later stage. The input cavity acts as the anode. If the total filament current is equal to 10 mA then the perveance at 3 kV is  $6.09 \times 10^{-8}$ . This value is less than or around  $10^{-8}$ , which is considered low enough to be able to ignore the effects of space-charge [22]. For such a relatively low voltage, low current gun, the development and operation of a tungsten filament is much simpler compared to the more complex “Pierce type” electron gun [23, 24]. The effect of ionizing rays (X-rays) can be neglected since the beam voltage is less than 40 kV [25].

The filament is bent into hairpin, forming an inverted ‘V’ shape. The diameter of the tungsten filament used is 0.22 mm. Two copper wires are used and are attached to the filament legs using screw terminals and screws. The mounting layout for the filament is shown below in Figure 7. The photo for the mounting layout for the tungsten filament is shown in Figure 8, while the photo for the mounting layout for the Thoria coated iridium filament is shown in Figure 9.

A circular nylon support base with 10.2 mm thickness and 31.2 mm diameter are used. Six holes are drilled on the nylon support base. A central hole is drilled in the middle of the nylon support base.

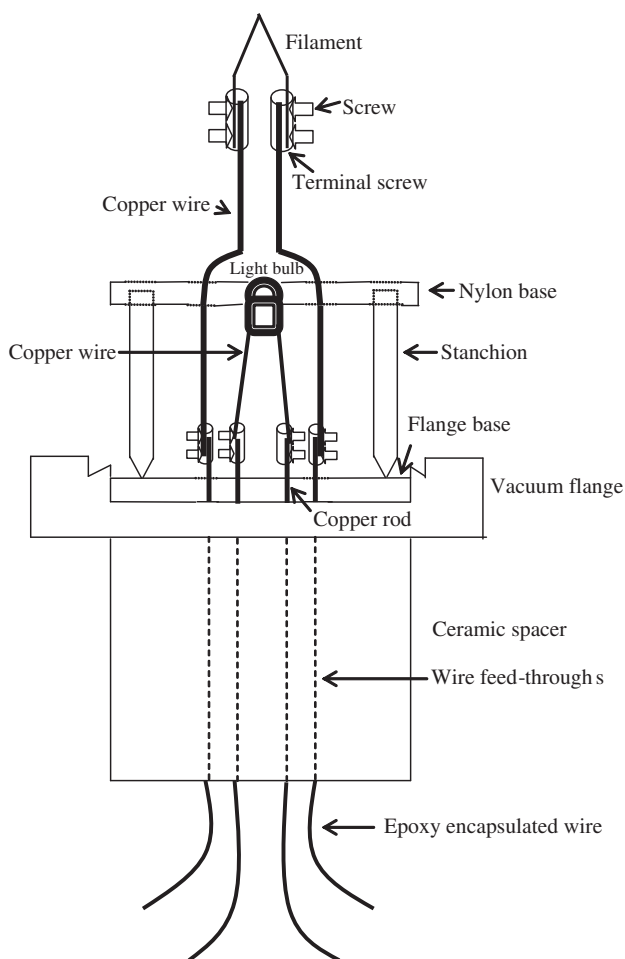


**Figure 7.** Filament mounting method using copper wires, screws and terminal screws.

The flange base section slot onto four stanchions fixed to the 70 mm diameter vacuum flange. In Figure 7, due to the diagram drawn in 2-D, only two stanchions are showed for simplicity purpose. The other ends of the stanchions are slotted onto the four holes on the nylon base. Hence, the function of the stanchions is to provide stability to the nylon support base and to hold it into stationery position. The stanchions are connected to earth, hence making the flange base section at earth potential. The presence of these holes on the nylon base also function to pump away efficiently gases generated during degassing.

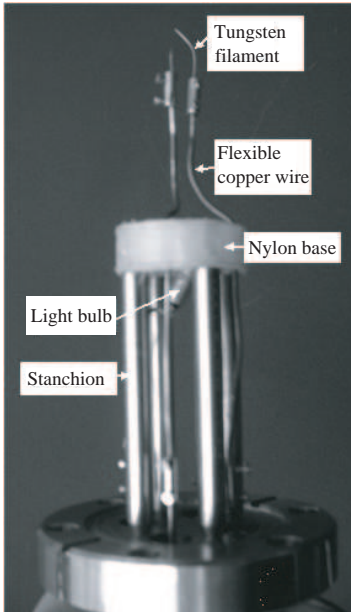


**Figure 8.** Photo of the mounting of the tungsten filament.

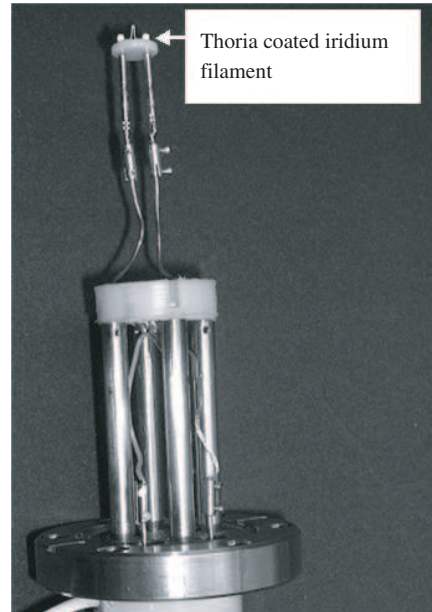


**Figure 9.** Photo of mounting of Thoria coated iridium filament.

The filament legs are attached to two copper wires. The copper wires are flexible and are fed directly from the flange base. From the flange base, the copper wires are then fed through the other two holes on the circular nylon base. Then they are bended by hand to form arc curves as shown in Figure 7 before being straightened again. The screw terminal can be now placed at the end of the copper wire, and screws are affixed to the filament legs. Ceramic beads are placed along the length of the copper wires to prevent electrical breakdown.

The filament's vertical position can be adjusted by sliding the terminal screws up and down respectively. The screws are used to attach the filament legs to the copper wires. The use of flexible copper wires is beneficial because they can be bended to adjust the filament's horizontal location. As a result, the filament is aligned correctly onto the middle of the aperture of the input cavity. It is clear that only about a millimetre or so of the filament (at the tip) contributes to the emission and the shape of the remainder of the filament is of no importance.

A small 2.5 Volts light bulb is also placed inside the inner hole of the nylon base. Two leads are soldered to this light bulb. The two leads are connected to a power supply. When 2.5 Volts are applied from the power supply, the light bulb will light up, therefore allowing the user to view the alignment of the filament tip in relation to the aperture of the input cavity. After the two cavities are placed on top of each other, separated by silicon 'O' ring, the light bulb is no more used (light up) during the experimental process.

The flange base has four protruding rods attached to it. Two rods are used to attach to the copper wires, while two other rods are used to attach to the leads connecting to the light bulb. Electrical connection leads from the grid and filament posts all pass separately through the vacuum flange via ready-made ceramic 'feed-throughs' welded in. Therefore, on the atmospheric side of the gun body, there are a total of 4 external leads encapsulated in a solid cylinder of epoxy. Two leads are for the two legs of the filament and the other two leads are connected to the light bulb. There is no internal lead specifically for the input cavity (anode connection). Hence an external ground wire is connected from earth to the outer wall (external surface) of the input cavity.

Clearly it would be desirable to have the filament to anode spacing at a minimum, since this would lead to less interception by the anode (depending on its aperture size) [23]. The distance between the tip of the filament and the input cavity aperture is 1 mm. If the filament is set too near or in the aperture, the emission current will be limited by space charge. This separation distance is sufficient to allow reliable operation at 3 kV without breakdown. The input cavity (anode) aperture size of 4 mm in diameter provides a low anode loss and avoids excessive diverging of the beam.

### 3.9. Electron Gun Circuit

The electron gun circuit can be seen in Figure 10. The filament is powered using a variac (variable auto transformer) and a step down filament transformer. The filament transformer used is the AT476 model from AWI Microwaves. The variac determines how much voltage will go to the step-down transformer. A bench top model of variac is used so as to bring up the filament current slowly. The output lines of the transformer are connected to the filament. This secondary winding of the transformer provides AC heating or filament voltage for filament of the electron gun.

The step down transformer reduces the incoming voltage to about 3 volts when current flows through it before reaching the filament. This

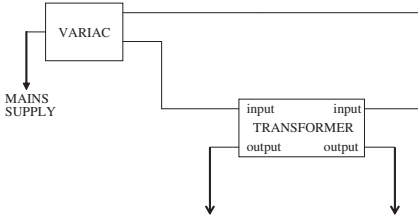


**Figure 10.** Electron gun circuit.

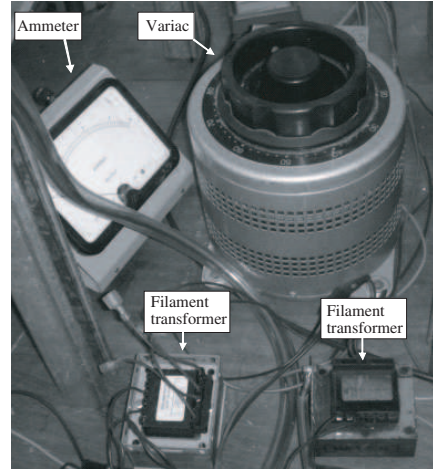


**Figure 11.** Photo of electron gun circuit.

results in a current of up to 5 Amperes flowing through the filament. The photo of the electron gun circuit is shown in Figure 11.

Electrical resistance causes the filament to heat up and release electrons by thermionic emission. The higher the current, the bigger the heat and the greater the number of electrons released. The filament requires high current and low voltage because the filament resistance is very low, i.e., if the voltage flowing through the filament is too high, the filament will burn up. Higher current requirements are met by setting the filament transformers in parallel, as shown in Figure 11. When a high voltage is applied between the filament (cathode) and input cavity (anode), all free electrons released from the filament surface are accelerated towards the anode.

### 3.10. Filament Material

At the initial stage, tungsten filament is used because it is readily available in the laboratory, and it is easy to make a ‘V’ shape tungsten filament. Tungsten wire is also available at a low cost and performed reasonably well. Tungsten filament has a high work function (4.55 eV). It requires around 4 Amps of current to heat it and for it to initiate electron emission. The tungsten filament that is available can produce maximum emission current of around 200  $\mu\text{A}$  at the tip. In order to produce greater than this current, another electron gun source need to be investigated.

Tungsten has the disadvantage of becoming very brittle (due to crystal growth) when it is heated, which means that it is easily broken by vibration. In addition it will instantly oxidise if exposed to atmospheric pressure while hot, resulting in the burn-out of the filament. The hot filament also generates CO and CO<sub>2</sub> in the vacuum system and causes larger gas molecules to be split into fragments. The solution is to investigate a filament material which is not easily oxidise, even when exposed to atmospheric pressure when hot. During the experimental process, the copper tubing need to be opened repeatedly to align the filament better to the aperture of the input cavity, after bringing up the vacuum pressure up to atmospheric pressure level. As a result, after several exposures to atmospheric pressure, the tungsten filament becomes more brittle and would eventually break. Hence a new 'V' shape tungsten filament has to be repeatedly constructed and placed on the studding.

An option is to use Thoria (thorium oxide) coated tungsten filament. This is just a tungsten filament, much like that in a light bulb, except that a tiny amount of the rare metal thorium was added to the tungsten. The free thorium is released within the thorium oxide coating during the heating of the filament (about 2400 degree Celsius). This free thorium migrates to the surface of the oxide coating and emits electrons. It is this free metal film of thorium on the surface of the oxide coating that results in the emission characteristics of the thorium coated filaments.

The tungsten filament with thorium is a much better producer of electrons than the plain tungsten filament by itself. This thoriated tungsten filament has a maximum emission current of 5 mA [26]. Thorium has a lower work function (3.41 eV) than tungsten. The Thoria coated tungsten filament can last a very long time, and is very resistant to high voltages. Although Thoria coated tungsten filament has a lower work function, it still has the brittle characteristic from the tungsten. A method must be investigated to lower the work function while investigating for a new material having non-burnout or non-brittle characteristic.

A solution is found by using Thoria coated iridium filament, as shown in Figure 12. Iridium has a high work function (5.27 eV) compared to tungsten. This high work function can be lowered by coating the iridium with Thoria which also results in longer filament life. The filament also requires less power and it can be operated at lower temperatures. This filament can produce maximum current emission of 20 mA, which is much greater than the tungsten filament.

Having a lower work function allows Thoria coated iridium filament to be very efficient at releasing electrons by thermionic

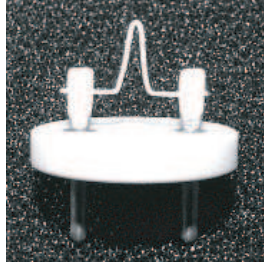


**Figure 12.** Photo of Thoria coated iridium filament.

emission. This means that it can operate at a lower temperature than tungsten to release the same number of ionising electrons. Experiment performed shows that only about 2 Amps of heating current is needed for it to start emitting electrons. This result in less CO and CO<sub>2</sub> produced and less molecular cracking. Unlike tungsten, iridium could also be operated in air at atmospheric pressure without bad effects.

A slight disadvantage of Thoria is the environmental issues due to the exposure to the alpha particles emitted by thorium. Hence, care must be taken in its handling and use. Iridium filaments are widely used in mass spectrometry, organic spectroscopy and X-ray sources and many are coated with thorium oxide to improve electron emission. The structure of this Thoria coated iridium filament is similar to the previously used tungsten filament, which is inverted 'V' shape.

#### 4. CONCLUSION AND FUTURE WORK

The design and analysis of pre-bunched free electron maser have been performed. Simulation results showed that the PFEM structure allows intense  $E$ -field strength to accumulate in the thin gap section of the cavity [9]. The resonant cavities are fine tuned using a phase shifter so that the electrons arriving at the output cavity will be in phase with the EM wave. The height of the thin gap section has been designed in such a way that the transit time of the electrons across the height of the thin gap section will be less than half of the EM wavelength. The strong  $E$ -field is expected to intersect with the in-phase electrons in the beam. Optimum energy exchange will occur and hence the output EM wave is expected to be significantly amplified.

The construction phase is now complete. Each of the main components has been evaluated as a separate module and testing of each component is now completed. The testing of the electron gun current emission has been performed, where the current flow across



the apertures of the output cavity was measured. Results showed that around 50% of the total filament current will flow across the apertures of the output cavity. The PFEM cavity construction was an important process of the research. The PFEM was constructed using affordable and available technologies. The construction of the main body of the PFEM was discussed, followed by the filament housing, the silica windows and the filament circuit housing. Methods used to tighten the two cavities were also presented, together with methods used to detect leaks in the system. The high vacuum system was also discussed in this paper. Due to the compactness of the PFEM system, a small vacuum system was used for pumping down the system to reach a vacuum condition. The next major component of PFEM is the electron gun. The design of electron gun was discussed in this paper, together with the electron gun circuit.

In the future, the output power of the PFEM will be raised to Watt level for industry demonstration purpose. At the initial stage, as described in this paper, the tungsten filament was used as a source of electron. The tungsten's emission from the tip is  $200\text{ }\mu\text{A}$  [24]. After gradually gaining confidence in the system, the next step is to use the Thorium coated iridium filament. The use of Thorium coated iridium filament was also discussed. The current emission used in the experiment is 10 mA. Hence 5 mA of beam current is expected assuming 50% of the total filament current flows across the apertures of the output cavity. The use of high voltage in the electron pre-bunching stage and high current source are expected to maximise the FEM gain and output considerably.

In the next step, a 'Pierce' type electron gun will be proposed for the PFEM system. The 'Pierce' type electron gun used by previous Free Electron Laser researcher produced a maximum emission current of 285 mA [27]. Hence, with the acceleration voltage of 3 kV, and the beam current of 142 mA (assuming 50% of the 285 mA current flow across the apertures of the output cavity), the resultant cavity PFEM output power will be significantly increased. In addition to that if a higher output power X-band source (23 dBm) will be used in the future, this will significantly further the cavity PFEM output power. However, emission at higher beam currents will also mean that space-charge spreading of the beam must be taken into consideration.

The *E*-field patterns and leakages near the apertures of the thin gap sections have been simulated using the CONCERTO software. Results showed that the aperture diameter of 1.5 mm produced an acceptable amount of leakages. Comparison of these results with the work done by Panda will be performed in the future [28]. The PFEM system design can be extended to higher frequencies by

scaling down the waveguide dimensions appropriately or increasing the acceleration voltage. Possible applications at frequencies above 30 GHz are millimetre wave imaging, treating of tumours and high resolution radar system [29–32].

## REFERENCES

1. Sabry, R. and S. K. Chaudhuri, “Formulation of emission from relativistic free electrons in a ring structure for electro-optical applications,” *Progress In Electromagnetic Research*, PIER 50, 135–161, 2005.
2. Pinhasi, Y. and Y. Lurie, “Generalized theory and simulation of spontaneous and super-radiant emissions in electronic devices and free-electron lasers,” *Phys. Rev. E*, Vol. 65, 026501.1–026501.8, 2002.
3. Arbel, M., A. Abramovich, A. L. Eichenbaum, A. Gover, H. Kleinman, Y. Pinhasi, and I. M. Yakover, “Superradiant and stimulated superradiant emission in a prebunched beam free-electron laser,” *Phys. Rev. Lett.*, Vol. 86, 2561–2564, 2001.
4. Vinokurov, N. A., *Proceedings of the International Conference on High Energy Charged Particle Accelerators*, Vol. 2, Serpukhov, Protvino, Russia, 1977.
5. Doria, A., R. Bartolini, J. Feinstein, G. P. Gallerano, and R. H. Pantell, “Coherent emission and gain from a bunched electron beam,” *IEEE J. Quantum Electron.*, Vol. 29, 1428–1436, 1993.
6. Ku, H. S. and T. Yusaf, “Processing of composites using variable and fixed frequency microwave facilities,” *Progress In Electromagnetics Research B*, Vol. 5, 185–205, 2008.
7. Tiwari, K. C., D. Singh, and M. K. Arora, “Development of a model for detection and estimation of depth of shallow buried non-metallic landmine at microwave X-band frequency,” *Progress In Electromagnetics Research*, PIER 79, 225–250, 2008.
8. Li, L. and C.-H. Liang, “Waveguide end-slot phased array antenna integrated with electromagnetic bandgap structures,” *Journal of Electromagnetic Waves and Applications*, Vol. 21, No. 2, 161–174, 2007.
9. Malek, F., J. Lucas, and Y. Huang, “Prototype design of compact and tuneable X-band pre-bunched free electron maser,” *Progress In Electromagnetic Research*, PIER 85, 1–23, 2008.
10. Gholami, M., “Analysis of output power delay in coaxial vircator,” *Progress In Electromagnetics Research B*, Vol. 4, 1–12, 2008.

11. Li, Z., T. J. Cui, and J. F. Zhang, "TM wave coupling for high power generation and transmission in parallel-plate waveguide," *Journal of Electromagnetic Waves and Applications*, Vol. 21, No. 7, 947–961, 2007.
12. Li, Z. and T. J. Cui, "Novel waveguide directional couplers using left-handed metamaterials," *Journal of Electromagnetic Waves and Applications*, Vol. 21, No. 8, 1053–1062, 2007.
13. Mondal, M. and A. Chakrabarty, "Resonant length calculation and radiation pattern synthesis of longitudinal slot antenna in rectangular waveguide," *Progress In Electromagnetics Research Letters*, Vol. 3, 187–195, 2008.
14. Paramesha, S. and A. Chakrabarty, "Waveguide as a near-field measuring probe of the two-element array radiator," *Progress In Electromagnetics Research B*, Vol. 7, 245–255, 2008.
15. Sjöberg, D., "Determination of propagation constants and material data from waveguide measurements," *Progress In Electromagnetics Research B*, Vol. 12, 163–182, 2009.
16. Mondal, M. and A. Chakrabarty, "Resonant length calculation and radiation pattern synthesis of longitudinal slot antenna in rectangular waveguide," *Progress In Electromagnetics Research Letters*, Vol. 3, 187–195, 2008.
17. Lim, K. S., V.-C. Kho, and T. S. Lim, "Design, simulation and measurement of a post slot waveguide antenna," *Journal of Electromagnetic Waves and Applications*, Vol. 21, No. 12, 1589–1603, 2007.
18. Mei, Z. L. and F. Y. Xu, "A simple, fast and accurate method for calculating cutoff wavelengths for the dominant mode in elliptical waveguide," *Journal of Electromagnetic Waves and Applications*, Vol. 21, No. 3, 367–374, 2007.
19. Cheng, Q. and T. J. Cui, "Guided modes and continuous modes in parallel-plate waveguides excited by a line source," *Journal of Electromagnetic Waves and Applications*, Vol. 21, No. 12, 1577–1587, 2007.
20. Dwari, S. A., A. Chakraborty, and S. Sanyal, "Analysis of linear tapered waveguide by two approaches," *Progress In Electromagnetics Research*, PIER 64, 219–238, 2006.
21. Al-Shamma'a, A. I., A. Shaw, R. A. Stuart, and J. Lucas, "Enhancement of an electron beam buncher for a CW FEM," *Nuclear Instruments and Methods in Physics Research*, Vol. 429, 304–309, 1994.
22. Han, J. E., M. Yoon, and S. Y. Park, "Design study of an electron

- gun for a high power microwave source,” *Journal of Korean Physical Society*, Vol. 44, No. 5, 1265–1268, May 5, 2004.
23. Dearden, G., E. G. Quirk, J. Lucas, and R. A. Stuart, “Industrial microwave FEL devices,” *Nuclear Instruments and Methods in Physics Research A*, Vol. 318, No. 1–3, 230–234, Elsevier, North-Holland, July 1992.
  24. Pierce, J. R., *Traveling-wave Tubes*, D. Van Nostrand Company, Inc., 1950.
  25. Oatley, C. W., “The tungsten filament gun in the scanning electron microscope,” *Journal of Physics E: Scientific Instruments*, Vol. 8, 1037–1041, June 23, 1975.
  26. Al-Shamma’a, A. I., “Enhancement of an electron beam buncher for a CW FEM,” *Nuclear Instrumentation and Methods in Physics Research A*, Vol. 429, 304–309, Elsevier, North-Holland, 1999.
  27. Wright, C. C., “Development of a free electron maser for industrial applications,” Ph.D. Thesis, Department of Electrical Engineering and Electronics, The University of Liverpool, 2000.
  28. Panda, D. K., A. Chakraborty, and S. R. Choudhury, “Analysis of co-channel interference at waveguide joints using multiple cavity modeling technique,” *Progress In Electromagnetics Research Letters*, Vol. 4, 91–98, 2008.
  29. Oka, S., H. Togo, N. Kukutsu, and T. Nagatsuma, “Latest trends in millimeter-wave imaging technology,” *Progress In Electromagnetics Research Letters*, Vol. 1, 197–204, 2008.
  30. Ibrahim, A. T., “Using microwave energy to treat tumors,” *Progress In Electromagnetics Research B*, Vol. 1, 1–27, 2008.
  31. Singh, G., “Analytical study of the interaction structure of vane-loaded gyro travelling wave tube amplifier,” *Progress In Electromagnetics Research B*, Vol. 4, 41–66, 2008.
  32. Mizuno, M., C. Otani, K. Kawase, Y. Kurihara, K. Shindo, Y. Ogawa, and H. Matsuki, “Monitoring the frozen state of freezing media by using millimetre waves,” *Journal of Electromagnetic Waves and Applications*, Vol. 20, No. 3, 341–349, 2006.